

Oscillation of adhering droplets in shear flow

Sebastian Burgmann^{1*}, Beawer Barwari¹, Uwe Janoske¹

¹Bergische Universität Wuppertal, Chair of Fluid Mechanics, Wuppertal, Germany

*burgmann@uni-wuppertal.de

Abstract

In this work the oscillation of adhering droplets in shear flow is analyzed for different fluid properties and droplet sizes. A water droplet of different volume (5 to 40 μl) and different portion of glycerine (0 to 50 %) is placed on a channel wall. Droplet height is less than 10 % of the channel height and therefore within the highest gradient of the velocity profile. Velocity of the channel flow is increased in each case from 0 to values at which the droplet detaches from the channel wall surface. Corresponding Reynolds numbers are up to $Re_{ch} = 10^4$. The droplet shape and contour deformation is analyzed by transmitted-light technique. For selected cases, the flow inside the droplet is measured by Particle-Image Velocimetry (PIV) using an infrared laser-diode and a CMOS-high-speed camera. The analysis of the temporal behavior of the droplet contour shows that the droplet oscillates with distinct peak frequencies. These frequencies can be associated with the first resonant frequency ω_R and half of that value. Additionally, frequencies of higher order modes appear for higher flow velocities. Increasing the amount of glycerine does not change the spectrum concerning the frequencies but changes the amplitudes: a significant damping of the oscillation can be observed. This damping effect can be directly linked with the increasing viscosity with increasing amount of glycerine. Additionally, this effect corresponds to an increase of the critical velocity that is needed to move the droplet. PIV measurements inside the oscillating droplet show that at low flow velocities in the temporal mean there is a clockwise rotation inside the droplet. For increasing incoming flow velocity in the temporal mean a second vortical structure appears at the downstream part which is counterclockwise rotating. This counterclockwise rotating structure becomes more dominant and the clockwise rotating structure seems to vanish for increasing velocity. The instantaneous flow structure inside the droplet is governed by vortical structures and a strong horizontal back- and forth-movement. These flow patterns appear regularly and can be correlated with the detected characteristic frequencies of the contour oscillation. Understanding the inner flow structure of oscillating droplets will help to improve the numerical modeling of these two-phase flows such that onset and droplet movement itself can be predicted more precisely.

1 Introduction

Condensed droplets or liquid sprays appear in many technical applications. These droplets may attach and adhere to the surfaces of the apparatus. It is possible, that there is an additional gas flow over these surfaces. Under critical conditions the initially adhering droplets may move. It is known from experience that droplets unexpectedly migrate to parts of the apparatus where they may lead to corrosion effects or electrical shortcuts. The specific critical conditions for such a droplet movement are not completely understood. Additionally, the prediction of droplet movement by means of numerical simulations is complex due to several problems e.g. modeling of contact angle hysteresis and surface tension force and undesired damping of the inner flow of the droplet (Maurer, 2017).

However, some general aspects are already known: larger adhering droplets in shear flow are deformed (Seevaratnam et al., 2010) and start to oscillate (Lin et al, 2006). These droplets stick to the surface until a critical flow velocity is reached and the droplet moves downstream still in contact with the surface. It is also known that this flow velocity at least depends on contact angle hysteresis and droplet volume (Fan et

al, 2011). In literature there is no common definition of the critical velocity: it might be the channel bulk velocity as in Fan et al. (2011) or in Maurer and Janoske (2015) or the local velocity of the shear flow profile at the maximum height of the droplet. Additionally, the droplet movement can be divided in several typical phases, e.g. movement of the advancing and/or receding contact line or gliding phase. The differentiation of these phases and especially the onset of the movement itself are hard to define. In our latest work a robust definition of the onset of droplet movement has been found (Barwari et al., 2018) and it has been pointed out that is advantageous to refer to the local velocity of the shear flow profile at the maximum height of the droplet for the definition of the critical flow velocity (Burgmann et al., 2017). However, the mechanisms of droplet instability for adhering droplets in shear flow are still insufficiently described. In this work we focus on the oscillation of the droplet contour and the arising instability of the inner flow structure of the droplet in shear flow.

2 Experimental set-up and methods

The liquid droplet behavior in a shear flow is analyzed in a Plexiglas-channel of rectangular cross-section at different flow velocities. A water droplet of different volume (5 to 40 μl) and different portion of glycerine (0 to 50 %) is placed on the bottom channel wall by a syringe. Volume flow rate of the air flow is defined by a mass flow controller. The channel length is sufficient to provide fully developed laminar or turbulent flow at the measurement section. The velocity profile at the location where the droplet will be placed is measured by hot-film anemometry (TSI 1750 CTA). Droplet height is less than 10 % of the channel height in each case, such that the droplet is within the strongest velocity gradient of the channel flow (fig. 1).

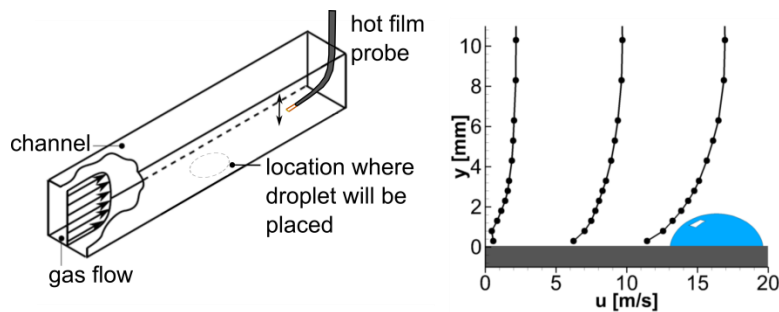


Figure 1: Experimental set-up for the investigation of the channel flow condition by means of hot-film anemometry (left) and corresponding velocity profiles for $Re_{ch} = 2.500, 12.400$ and 22.200 , respectively, also showing a typical droplet size (right).

The air flow rate is continuously increased in a single measurement until the droplet starts to move and is transported downstream. The temporal droplet behavior is measured by high-speed visualization using transmitted-light technique: a LED illuminates the droplet from the back such that a high-speed camera (MotionBLITZ EoSens Cube7) records the shadow of the droplet. Hence, images of the droplet provide a strong contrast for the application of an edge-detection algorithm. A Fast Fourier Transformation (FFT) is applied on the time-dependent contour position such that the droplet oscillation and the corresponding frequencies can be analyzed. The increase of the glycerine ratio up to 50 % only significantly alters the viscosity μ (+477 %) but only slightly density ρ (+13 %) and surface tension σ (-9 %). Hence, the supposed damping effect of the viscosity on the oscillation can be studied.

For selected cases, Particle-Image Velocimetry (PIV) is applied to analyze the flow inside the droplet. The PIV-system consists of an infrared laser-diode with $\lambda = 805$ nm and 50 W electrical power in cw-mode. Laser light is focused and formed to a thin light sheet (1 mm thickness) by a lens-system. The tracer particles (polystyrol) with a mean diameter of 4.2 μm are premixed into the water which is used to form the droplet. An 8 bit HCC1000 CMOS-high-speed camera with 1.024×1.024 pixels is used. The modular c-mount zoom-lens of the camera has a low focal depth, such that the particles in the center plane of the droplet are in focus, although the light sheet is relatively thick. Particles on the droplet surface are out-of

focus and can be eliminated by image processing. In the PIV measurements 1.024 image pairs are recorded in each case. For each image pair PIV post-processing is performed using a scheme of adaptive cross-correlation and an interrogation window size of 32 px with 50 % overlap.

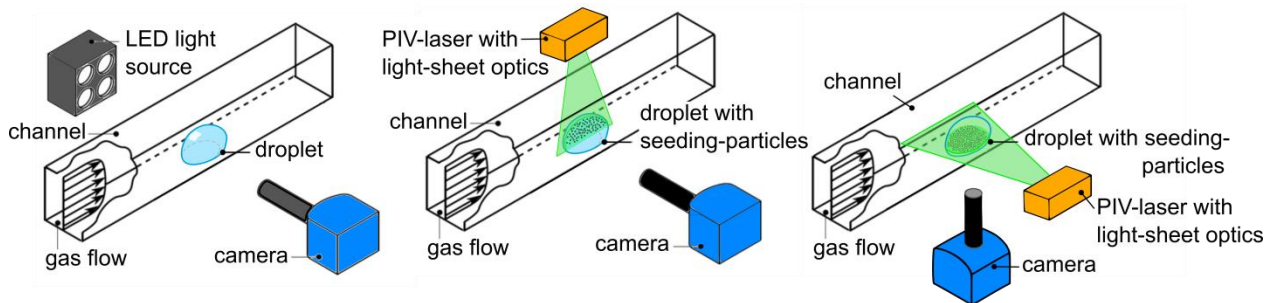


Figure 2: Experimental set-up for the investigation of the contour oscillation (left) and the inner flow structure of the droplet by means of PIV(center and right)

3 Results

The analysis of the temporal behavior of the droplet contour shows that the typical shape of the non-moving and moving droplet is not significantly altered within the investigated range of glycerine-content (0 to 50 %). Contour-images show a typical mean deformation of the droplet in a way that the center of gravity is shifted downstream and the upstream part of the droplet exhibits a flat curved shape whereas downstream the contour becomes steeper (fig. 3). Further details can be found in Barwari et al. (2018).

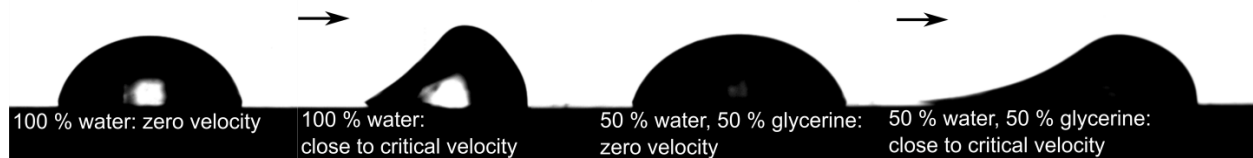


Figure 3: typical shape of a 23,4 µl droplet without and with shear flow for pure water droplets (left) and droplets of 50 % water and 50 % glycerine (right)

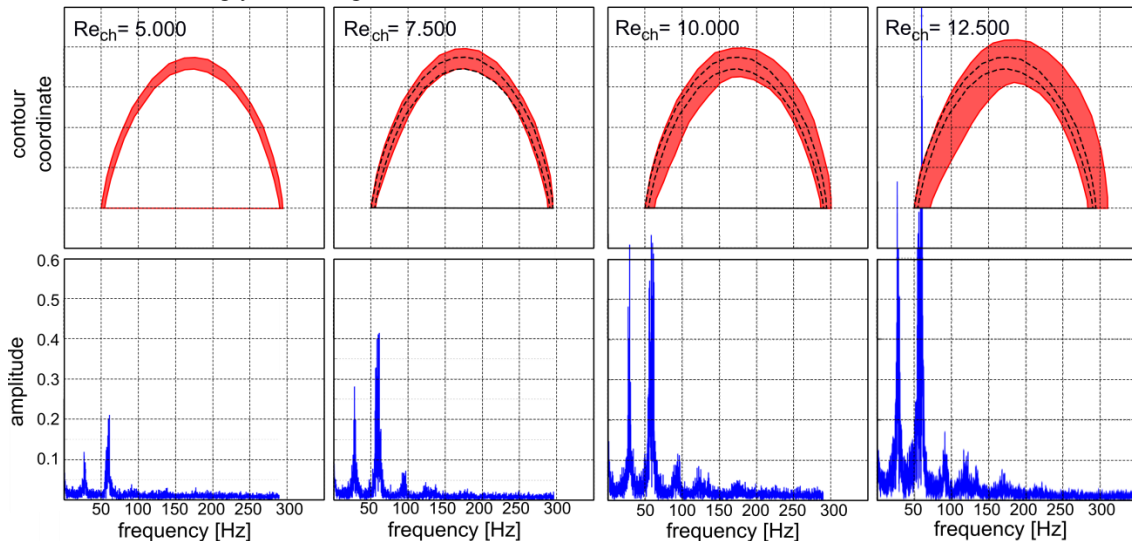


Figure 4: Contour oscillation and characteristic frequency spectra for an oscillating 20 µl water droplet in a shear flow for channel flow of 35 %, 52 % 70 % and 87 % of the critical velocity (left to right)

The oscillation of the droplet contour is recorded and analyzed by FFT. It was found that the droplet starts to oscillate with an up- and down-movement and additionally with a back- and forth-movement. As indicated in fig. 4, the temporal mean contour is shifted in a way that the center of gravity moves

downstream for increasing channel flow velocity. The bandwidth of contour position is indicated by the broad red band. However, the up- and down-movement and the back- and forth-movement still co-exist for the stronger deformed droplet. It was found that the oscillations in x- and y-direction possess the same spectra. The spectra reveal distinct peak frequencies. These frequencies can be associated with the first resonant frequency ω_R and half of that value according to the formula given by Lamb (1932) with l being an integer value of 2 or higher, σ and m are the surface tension and mass of the drop, respectively.

$$\omega_R = \sqrt{\frac{\sigma}{3\pi m} l(l-1)(l+2)} \quad (1)$$

Although this formula initially was given for a free droplet, it seems to be applicable for adhering droplets of almost spherical cap-shape.

Interestingly, the spectra do not change concerning the resonant frequency ω_R when the shear flow velocity increases: the amplitudes rise but the dominant frequency peaks remain. But frequencies of higher order modes ($l=3$ and $l=4$) appear for higher flow velocities (fig 4). Increasing the amount of glycerine does not change the spectrum concerning the frequencies but changes the amplitudes: a significant damping of the oscillation can be observed (fig. 5). The damping of the droplet oscillation corresponds to an increase of the critical velocity that is needed to move the droplet as shown in Barwari et al. (2018).

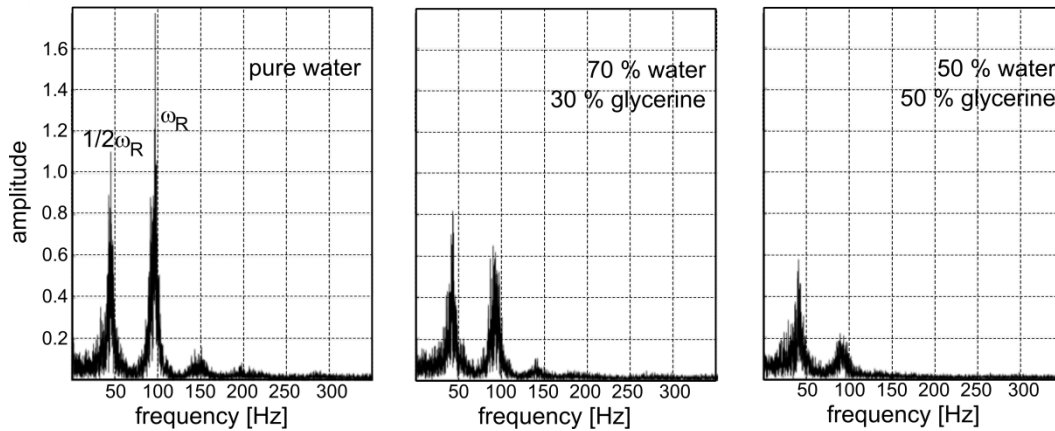


Figure 5: Frequency spectra for an 8 μl droplet of different ratio of water/glycerine showing the damping effect of the viscosity and the independence of the oscillation frequencies on viscosity

PIV measurements inside an oscillating 20 μl water droplet show that at low flow velocities, i.e. approximately 20 % of the critical velocity, in the temporal mean there is a clockwise rotation inside the droplet (channel flow from the left). For increasing channel flow velocity in the temporal mean a second vortical structure appears at the downstream part which is counterclockwise rotating (fig. 6). This counterclockwise rotating structure becomes more dominant and the clockwise rotating structure seems to vanish for increasing velocity. Interestingly, the mean flow structure in a horizontal measurement plane is also completely changed: in each investigated case there are two counter-rotating structures leading to a strong flow at the edge of the droplet and a counter-movement in the center. For increasing channel flow velocity the rotation direction of the two vortical structures changes completely (fig. 6).

Analyzing the temporal change of the flow inside the droplet shows that there are clockwise rotating structures moving from the front to the back part of the droplet. Additionally a strong horizontal back and forth movement is observed. These flow patterns appear regularly and can be correlated with the detected characteristic frequencies of the contour oscillation. The movement of the clockwise rotating vortex inside the droplet seems to correspond to $1/2 \omega_R$ whereas the strong lateral back- and forth-movement corresponds to ω_R . For higher channel flow velocities more unstructured flow pattern appear. Interestingly, although the temporal mean flow field completely changes when the flow velocity is increased, the contour frequency spectrum does not significantly change. Only higher order modes appear that might be

linked to the unstructured flow pattern observed in PIV results. There is a need for further analysis and measurements.

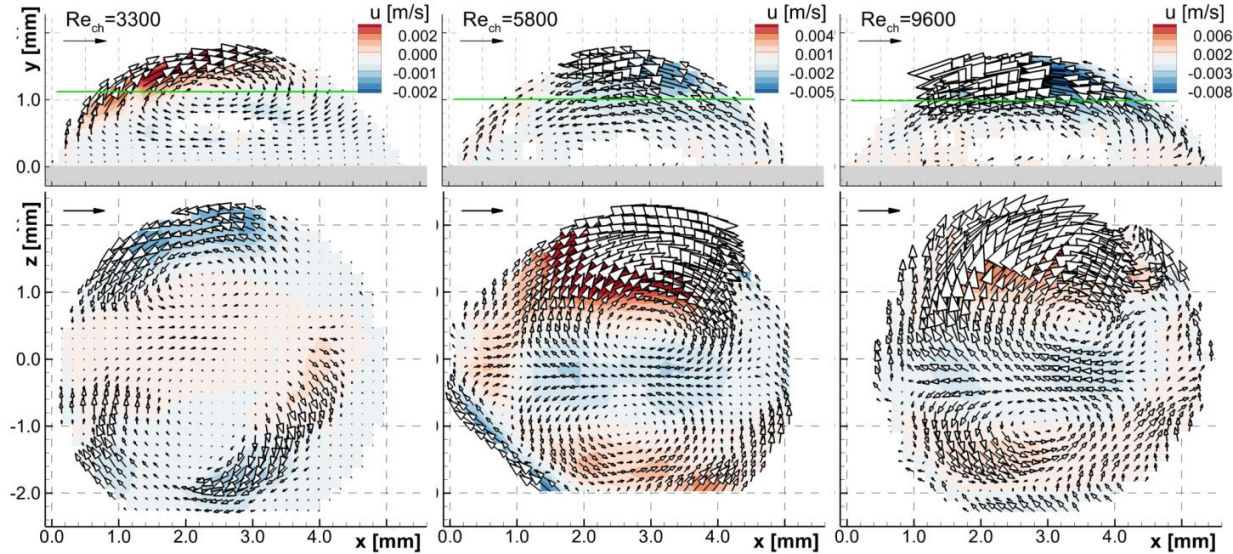


Figure 6: Temporal mean velocity field inside an oscillating 20 μl water droplet for increasing channel flow velocities (left to right: 23 %, 41 % and 68 % of the critical velocity). Top: side view, bottom: bottom view

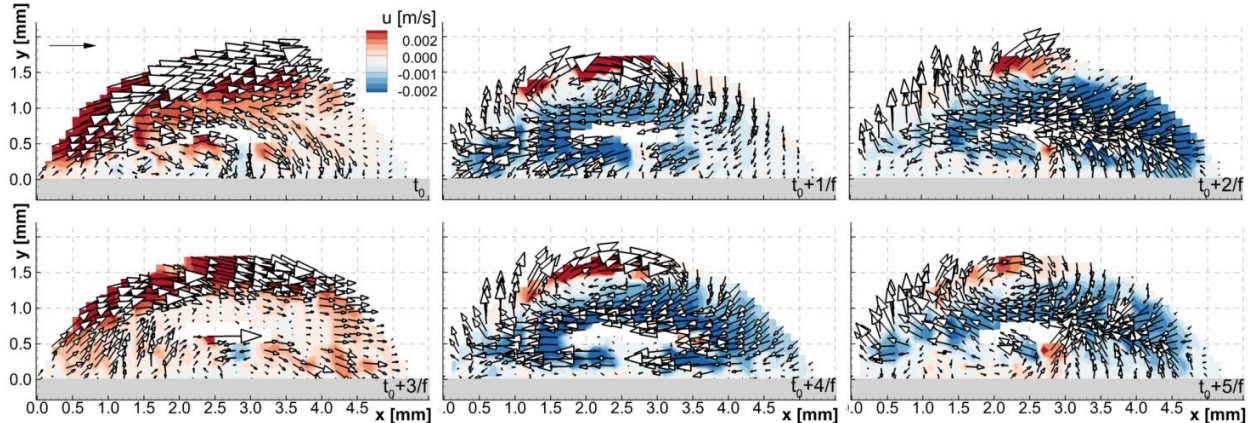


Figure 7: Instantaneous velocity field inside an oscillating 20 μl water droplet at 23 % of the critical velocity showing the repeating pattern of the downstream movement of the clockwise rotating vortex (recording frequency $f = 115 \text{ Hz}$) resulting in a frequency of $1/2 \omega_R$

4 Conclusion

Adhering droplets in shear flow start to oscillate before the flow velocity is high enough to move the droplet. In this work a deeper insight into the droplet instability is gained. It has been shown that the almost spherical-cap shaped droplet oscillates with distinct peak frequencies that can be associated with the resonant frequency ω_R of a spherical droplet of the same volume. Changing the ratio of water and glycerine of the droplet-fluid only significantly changes the viscosity. Hence, based on the present data it can be stated, that the oscillation frequency only depends on the droplet volume and surface tension but not the viscosity. However, for increasing viscosity a significant damping of the oscillation can be observed. This damping effect can be directly linked with the increase of the critical velocity that is needed to move the droplet. It has been observed that for higher channel flow velocities frequencies of higher order modes appear for higher flow velocities. PIV measurements have been performed to analyze the inner flow structure of the oscillating droplet and to link that flow structure with the contour oscillation. It has been found that the inner flow structure in the center plane is dominated by a clockwise

rotating vortex which periodically moves downstream with $1/2 \omega_R$. A strong back- and forth-movement with ω_R was found. Obviously, this second flow pattern dominates for increasing flow velocity since the amplitude of this frequency rises significantly. In the temporal mean the combination of the clockwise rotating vortex and the back- and forth-movement leads to a flow pattern inside the droplet which looks like a strong counter-clockwise rotating vortex. Additional measurements from the bottom of the channel also reveal a reverse of the rotational flow structure.

PIV-measurements from below through the wall are applicable when this wall can be made transparent as in this case and also demonstrated by e.g. Marin et al. (2016) for non-moving evaporating droplets. When the wall is non-transparent, e.g. a porous wall, this optical access cannot be provided. Hence, PIV measurements have to be performed through the curved surface of the droplet. As shown by Minor et al. (2009) for a non-oscillating droplet in shear flow, the precision of the measurement of the inner flow structure of the droplet can be increased using ray-tracing methods. The oscillating contour of the droplet in this case hinders the application of a ray-tracing correction. Hence, the results presented here only show typical pattern of the flow inside an oscillating droplet. Precise measurements may be possible using fast adaptive optics that correct the distortion of the droplet surface (Teich et al., 2016, 2017). Additional measurements are planned using these techniques. Understanding the inner flow structure of oscillating droplets will help to improve the numerical modeling of these two-phase flows such that onset and droplet movement itself can be predicted more precisely.

References

- Barwari B, Burgmann S, Janoske U (2018) Deformation and movement of adhering droplets in shear flow. *5th Int. Conf. on Experimental Fluid Mechanics*, July 2-4, Munich, Germany
- Burgmann S, Barwari B, Maurer T, Janoske U (2017) Hydrodynamic instabilities of a droplet on a plate influenced by flow and vibration. *Symposium "Lasermethoden in der Strömungsmesstechnik"*, September 5-7, Ettlingen, Germany
- Fan J, Wilson M, Kapur N (2011) Displacement of liquid droplets on a surface by a shearing air flow. *Journal of Colloid and Interface Science*, 356(1): 286–292
- Lamb H (1932) *Hydrodynamics*. Cambridge University Press, UK
- Lin Z, Peng X, Wang X (2006) Oscillation characteristics of droplets on solid surfaces with air flow. *Heat Transfer - Asian Research*, 35(1): 13–19
- Marin A, Liepelt R, Rossi M, Kähler CJ (2016) Surfactant-driven flow transitions in evaporating droplets. *Soft Matter*, 12, 1593-1600
- Maurer T (2017) Experimentelle und numerische Untersuchung der Tropfenbewegung unter Einfluss von äußeren Kräften. *Dissertation, Reports of the Chair of Fluid Mechanics*, 978-3-8440-5135-3, Shaker Verlag, Germany
- Maurer T, Janoske U (2015) Experimental study of water drop motions induced by superposition of vibrations and shear flows. *Computational Methods in Multiphase Flow VIII*, 89: 399-409
- Minor G, Djilali N, Sinton D, Oshkai P (2009) Flow within a water droplet subjected to an air stream in a hydrophobic microchannel. *Fluid Dynamics Research*, 41, 045506
- Seevaratnam GK, Ding H, Michel O, Heng JYY, Matar OK (2010) Laminar flow deformation of a droplet adhering to a wall in a channel. *Chemical Engineering Science*, 65(16): 4523-4534
- Teich M, Mattern M, Sturm J, Büttner L, Czarske JW (2016) Spiral phase mask shadow-imaging for 3D-measurement of flow fields. *Opt. Express* 24, 27371–27381
- Teich M, Sturm J, Büttner L, Czarske JW (2017), Distortion-free 3D imaging using wavefront shaping. *Proceedings of SPIE - The International Society for Optical Engineering* Vol. 10335